

Results of a Long-Term Monitoring of the 1.35-cm Water–Vapor Maser Source ON 1 (1981–2013)

E. E. Lekht^{1*}, V. V. Krasnov², and A. M. Tolmachev²

¹*Lomonosov Moscow State University,
Sternberg Astronomical Institute, Universitetskii pr. 13, Moscow, 119992 Russia*

²*Pushchino Radio Astronomy Observatory, Astropace Center, Lebedev Physical Institute,
Russian Academy of Sciences, Pushchino, Moscow oblast, 142292 Russia*

Received March 14, 2014

Abstract—We present the results of our long-term monitoring of the 1.35-cm water–vapor maser source ON 1 performed at the 22-m radio telescope of the Pushchino Radio Astronomy Observatory from 1981 to 2013. Maser emission was observed in a wide range of radial velocities, from -60 to $+60$ km s⁻¹. Variability of the integrated flux with a period of ~ 9 years was detected. We show that the stable emission at radial velocities of 10.3, 14.7, and 16.5 km s⁻¹ belongs to compact structures that are composed of maser spots with close radial velocities and that are members of two water-maser clusters, WMC 1 and WMC 2. The detected short-lived emission features in the velocity ranges from -30 to 0 and from 35 to 40 km s⁻¹ as well as the high-velocity ones are most likely associated with a bipolar molecular outflow observed in the CO line.

DOI: 10.1134/S1063773714080052

Keywords: *star-forming regions, maser sources, water–vapor lines.*

INTRODUCTION

The source ON 1 in Cygnus is associated with a dense molecular cloud and an ultracompact H II region (Zheng et al. 1985; Argon et al. 2000) having a centimeter-continuum luminosity $\geq 10^{4.2} L_{\odot}$, implying the spectral type B0 for the exciting star (McLeod et al. 1998). This source exhibits clear evidence of on-going star formation: a high-density gas, numerous high-velocity outflows, water–vapor (Turner et al. 1970; Sullivan 1970; Genzel and Downes 1977) and hydroxyl (Fish et al. 2005) masers, and near-infrared sources. A far-infrared point source is also located here (Kumar et al. 2004). According to the most reliable estimates, the distance to ON 1 is 1.8 kpc (see, e.g., McLeod et al. 1988; Kumar et al. 2004).

VLBI observations have shown that the H₂O emission is concentrated in two clusters: the northern WMC 1 and the southern WMC 2 (Downes et al. 1979; Nagayama et al. 2008). The clusters are 2'' (3600 AU) away from the UC H II region observed in continuum at 8.4 GHz and are spaced 1.6'' (2900 AU) apart in the northeast–southwest (NE–SW) direction. Two submillimeter continuum sources, SMA 1 and SMA 2 (Su et al. 2004), associated precisely with these two H₂O maser clusters

(Nagayama et al. 2008) were found at 345 GHz, and all these objects are collectively considered as a cluster of young stellar objects.

Numerous gas outflows were detected in the same ON 1 region (Kumar et al. 2004; Nagayama et al. 2008). A bipolar outflow in the $J = 2-1$ CO line near WMC 1 in the E–W direction (Kumar et al. 2004) with an expansion velocity of 69 ± 11 km s⁻¹ (Nagayama et al. 2008) stands out among them. The proper motions of maser features in the northern cluster are associated with this outflow. Another bipolar outflow was detected in the NH₃ and H¹³CO lines at a velocity of 4.5 km s⁻¹ in the NE–SW direction. Although this outflow is interpreted by some authors as a rotating ring or disk (Zheng et al. 1985; Lim and Ho 2002), based on their NH₃ line observations, Kumar et al. (2004) still give preference to the model of an outflow.

Nagayama et al. (2008) point out that the process of star formation in ON 1 propagates from the western side of the UC H II region to the eastern side of both maser clusters. They surmise that the northern source (the northern cluster of maser spots and the young star) form with the UC H II region a binary system with a relative velocity $\Delta V_{\text{LSR}} = 3$ km s⁻¹ and a total mass of $\sim 37 M_{\odot}$. The hydroxyl maser emission is also associated with the UC H II region, with its

*E-mail: lekht@sai.msu.ru

sources being located mainly at the periphery of this region (Forster et al. 1978).

The H₂O maser activity manifests itself in a wide range of radial velocities (from -80 to $+60$ km s⁻¹), but mainly in the central part of the spectrum, in the range 4 – 18 km s⁻¹. Maser emission with a peak intensity exceeding 600 Jy was also recorded here (Turner et al. 1970; Lekht et al. 1995).

OBSERVATIONS AND DATA ANALYSIS

Our observations of the H₂O maser source at 1.35 cm in the ON 1 region ($\alpha_{1950} = 20^{\text{h}}8^{\text{m}}10^{\text{s}}$, $\delta_{1950} = 31^{\circ}22'39''$) were carried out at the RT-22 radio telescope of the Pushchino Radio Astronomy Observatory from 1981 to 2013 with a mean interval between the observations of 1.8 months. In 1993 and 1994, the observations were conducted, on average, every five months, while no observations were conducted in the time intervals May 2006–January 2008 and August 2008–March 2009 for technical reasons.

The system noise temperature was 200 – 300 K and, beginning in 2005, 100 – 200 K, depending on the weather conditions. The antenna beamwidth at 1.35 cm is $2.6'$. The antenna sensitivity for unpolarized emission is 25 Jy K⁻¹. To minimize the influence of the possible polarization of the measured signal on the measured intensity, we tried to observe the source at approximately the same position angle. Note that continuum sources with a well-known absolute intensity (Jupiter, Venus, DR-21) are occasionally observed to calibrate the received signals at RT-22. These observations showed that the effective area of the antenna (its sensitivity) remained constant in all these years if, of course, the signal absorption in the Earth's atmosphere under different meteorological conditions is properly taken into account during the observations. Note also that an important factor in measuring the signal is the accuracy of the telescope's automatic pointing at the source; to control this accuracy, before the beginning of our observations, we almost always adjusted the antenna based on maser sources with a high intensity: Orion KL, W 49 N, W 3 OH.

The antenna is pointed at a strong source, the peak of its emission is found, the actual position of the source is compared with the calculated one, and the pointing correction found in this way is applied during the subsequent observations of the sources to be studied. In this way, an accuracy of automatic pointing at the source of 7 – 10 arcsec (if there is no lateral heating of the antenna by the Sun) can be achieved.

In 1981–2004, the signal was analyzed by a 128-channel filter-type spectrum analyzer with a resolution of 0.101 km s⁻¹. A 2048-channel autocorrelation

spectrum analyzer with a resolution of 0.0822 km s⁻¹ has been used since 2005. This allowed us to conduct observations in a wide range of radial velocities and, in particular, to record high-velocity emission in ON 1.

Selected H₂O spectra in ON 1 was published in 1995 (Su et al. 2004). Figure 1 presents all of the spectra taken over the observed period. The radial velocity relative to the local standard of rest in km s⁻¹ is along the horizontal axis and the flux density in Jy is along the vertical axis. The vertical arrow indicates the scale in Jy. The dashed lines indicate the emission features that cross the higher-lying spectra.

Since we have performed our observations in a wide range of radial velocities only after the 2048-channel autocorrelation spectrum analyzer was put into operation in 2005, we analyzed the variability of the integrated flux for the entire monitoring only for the range of radial velocities 4 – 18 km s⁻¹. Figure 2 shows a plot of the integrated-flux variability. The dashed line indicates the slow flux variations. The main maxima are marked by the vertical solid arrows and are numbered for convenience. The additional (secondary) maxima are marked by the dotted arrows.

DISCUSSION

The H₂O spectra toward the source ON 1 have mainly a triplet structure, i.e., emission at low radial velocities and high-velocity emissions with red and blue shifts. The emission features are identified with the two clusters of maser spots and the bipolar outflow observed in the CO line.

Identification

The most intense and stable H₂O maser emission features are shown in Fig. 3. We also included the data from Nagayama et al. (2008) (open circles). According to Downes et al. (1979) and Nagayama et al. (2008), the emission features are identified with the northern source WMC 1 in the range of radial velocities 12 – 17 km s⁻¹ and with the southern source WMC 2 in the ranges 5.9 – 12 and 17.5 – 23 km s⁻¹. Of course, there are weak features that slightly disrupt this separation, but they barely affect the overall picture. The belonging of features to the corresponding clusters is shown in Fig. 3.

The emission at large negative velocities was first detected by Genzel and Downes (1977). However, because of the low flux level, it was not identified. Kurtz and Hofner (2005) observed the emission in ON 1 in a wider range of radial velocities, from -53 to $+63$ km s⁻¹. Felli et al. (2007) monitored ON 1 in 1987–2007. The high-velocity emission, with both blue ($V_{\text{LSR}} < -20$ km s⁻¹) and red ($V_{\text{LSR}} >$

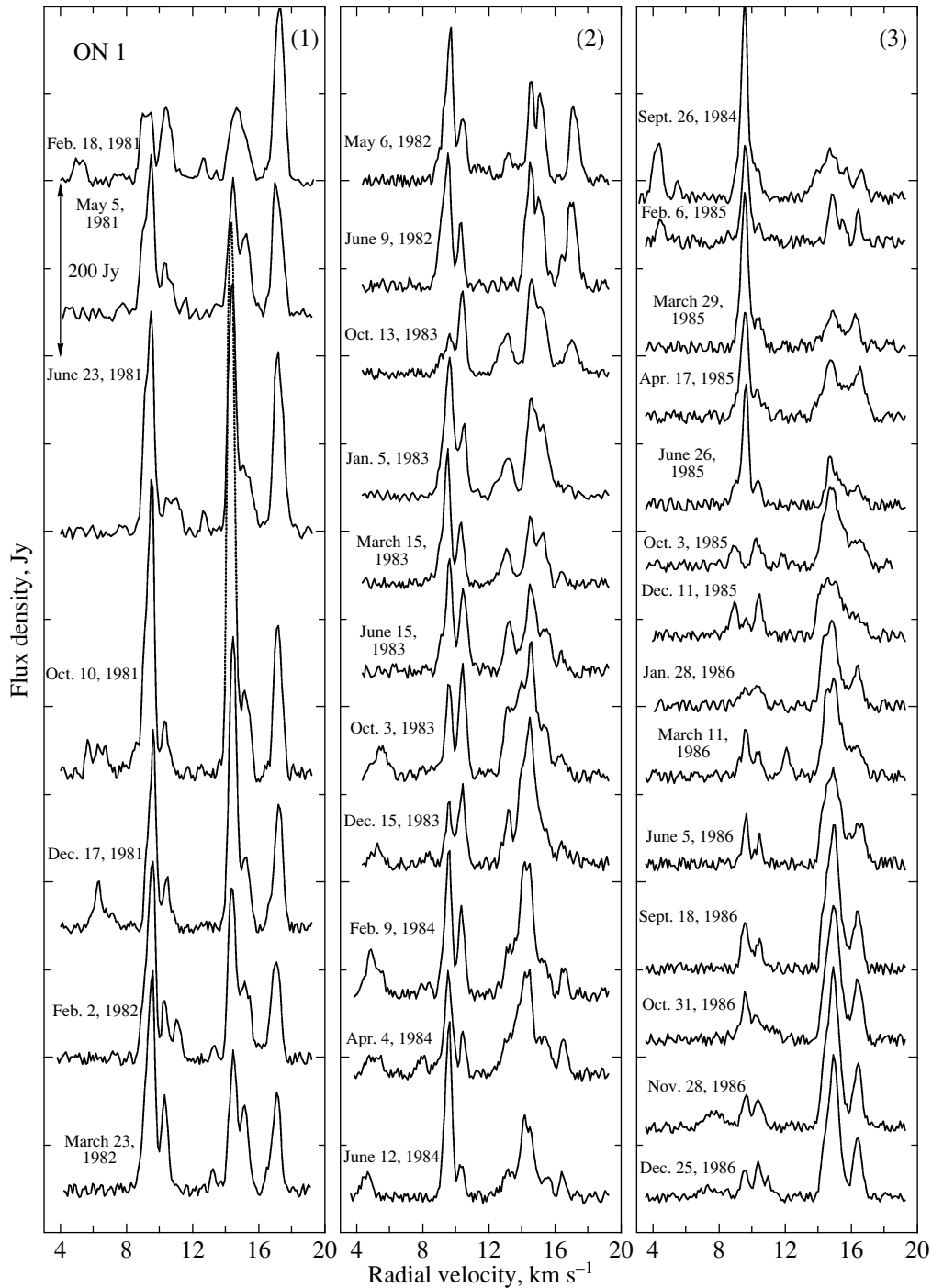


Fig. 1. H₂O maser emission spectra toward the source ON 1. The double arrow indicates the scale. The radial velocity is given relative to the local standard of rest.

35 km s⁻¹) shifts, was identified in 2005–2006, when the emission was fairly intense (Nagayama et al. 2008). All these high-velocity features are in the northern source and are associated with the submillimeter source SMA 1 and with the outflow observed in the CO line. The high-velocity emission and its evolution carry important information about the pro-

cesses occurring during the formation of young stellar objects in ON 1.

Maser Emission Variability

As we have already pointed out, the high-velocity emission is associated mainly with the bipolar outflow

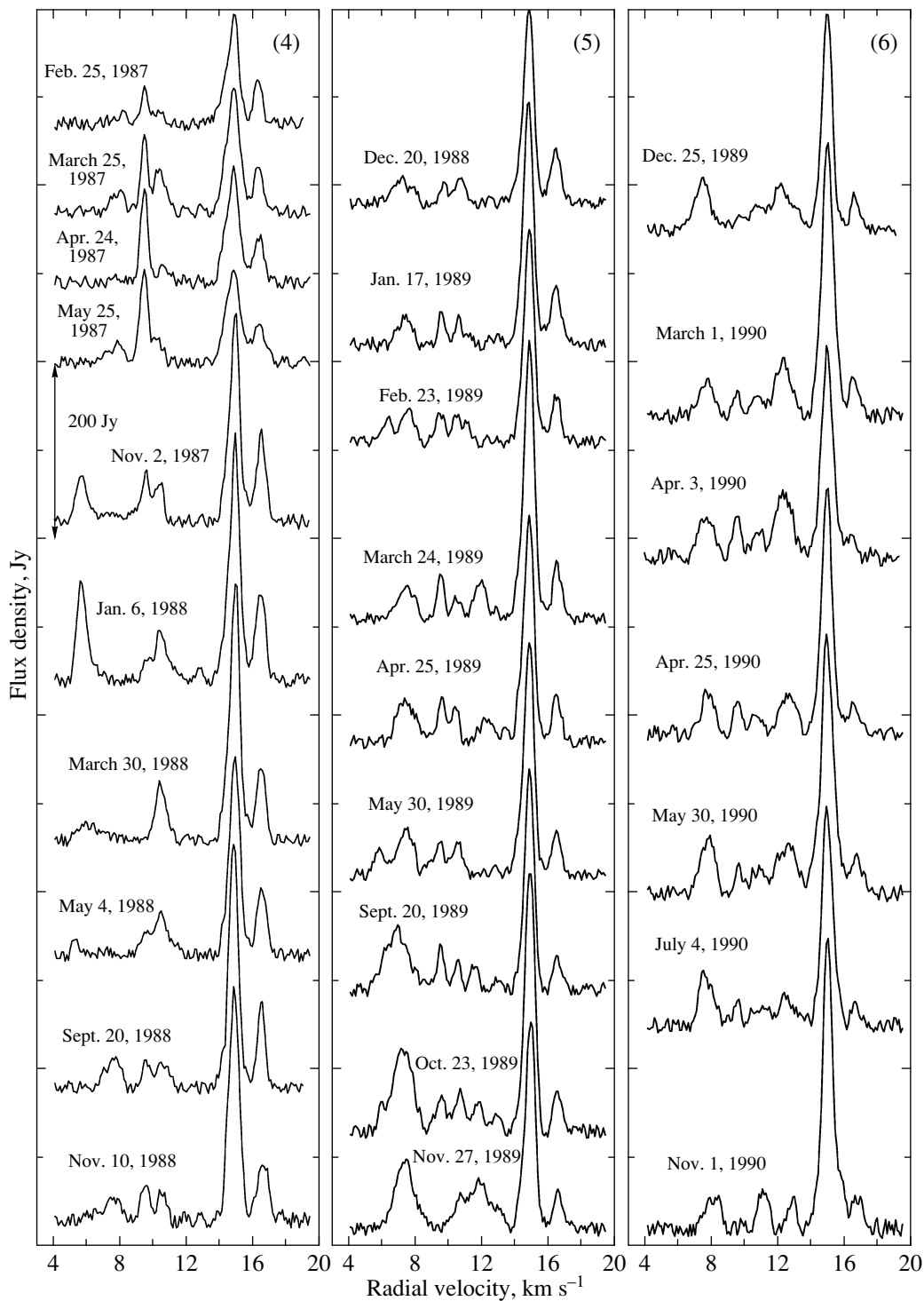


Fig. 1. (Contd.)

of matter, while the emission in the velocity range 4–18 km s⁻¹ is associated with the clusters of maser spots WMC 1 and WMC 2. An important parameter of the maser emission is its integrated flux. It reflects the state of the entire maser, and not just its individual features. The variability of the integrated flux calcu-

lated in the range of radial velocities 4–18 km s⁻¹ is shown in Fig. 4. The long-period variability component was identified (dotted line). The mean period is ~8.9 years.

For each maximum, we constructed the average spectra (see Fig. 5). The averaging time intervals

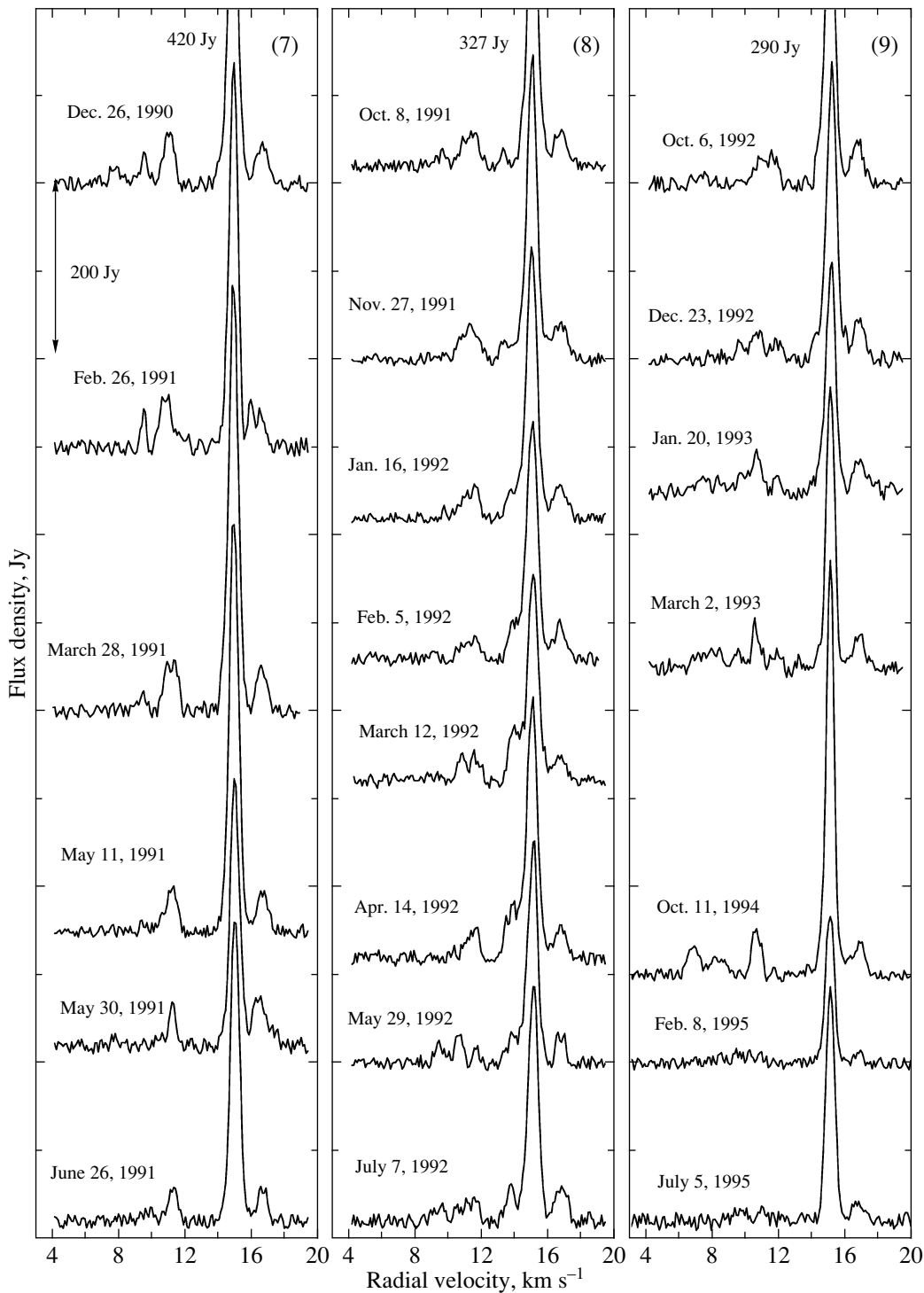


Fig. 1. (Contd.)

were taken near the maxima. A close similarity between the average spectra is observed for the 1990 and 1998 maxima, especially at radial velocities of 14.7 and 16.5 km s^{-1} . This emission is identified with the cluster of maser spots WMC 1. Figure 5 also shows the average spectrum near the emission min-

imum of 2003–2005 (dotted line). A close similarity of this spectrum to the average spectra at the maxima (curves 2 and 3) is also observed.

Additional maxima were occasionally superimposed on the main maxima. As a rule, they were observed near the main maxima (before and after

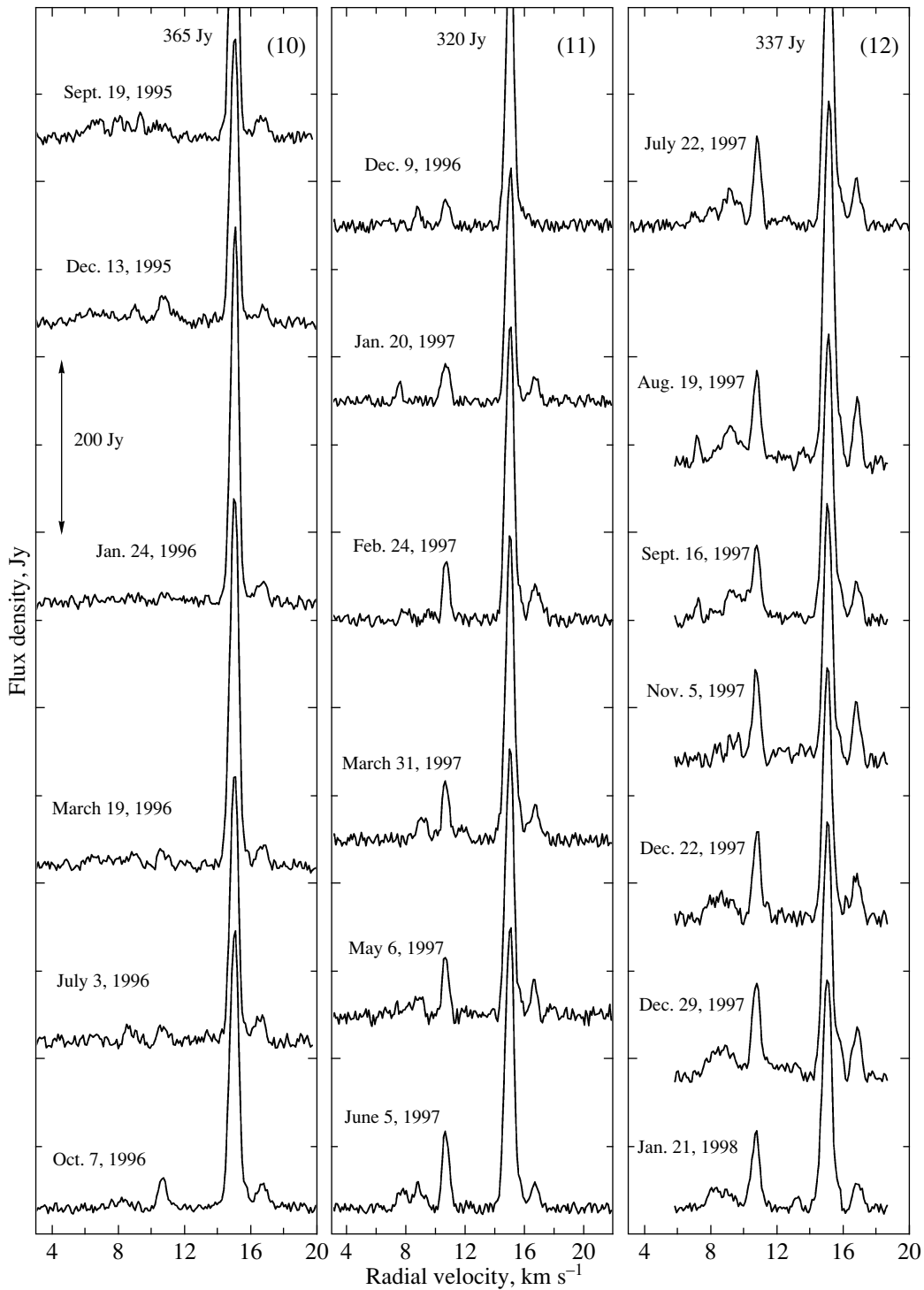


Fig. 1. (Contd.)

them). Two short-lived bursts of the integrated flux in 2010 and 2012 were caused only by short flares of emission at velocities of 7.9 and 14.9 km s⁻¹, respectively.

Figure 6 shows the flux density variability for the main emission features. It is these features and es-

pecially the component at 14.7 km s⁻¹ that make a major contribution to the integrated-flux variability. During the 1985 and 2005 minima, all components had emission minima. In contrast, at the 1995 minimum, the feature at 9.5 km s⁻¹ had an emission maximum. The picture was also similar for all maxima

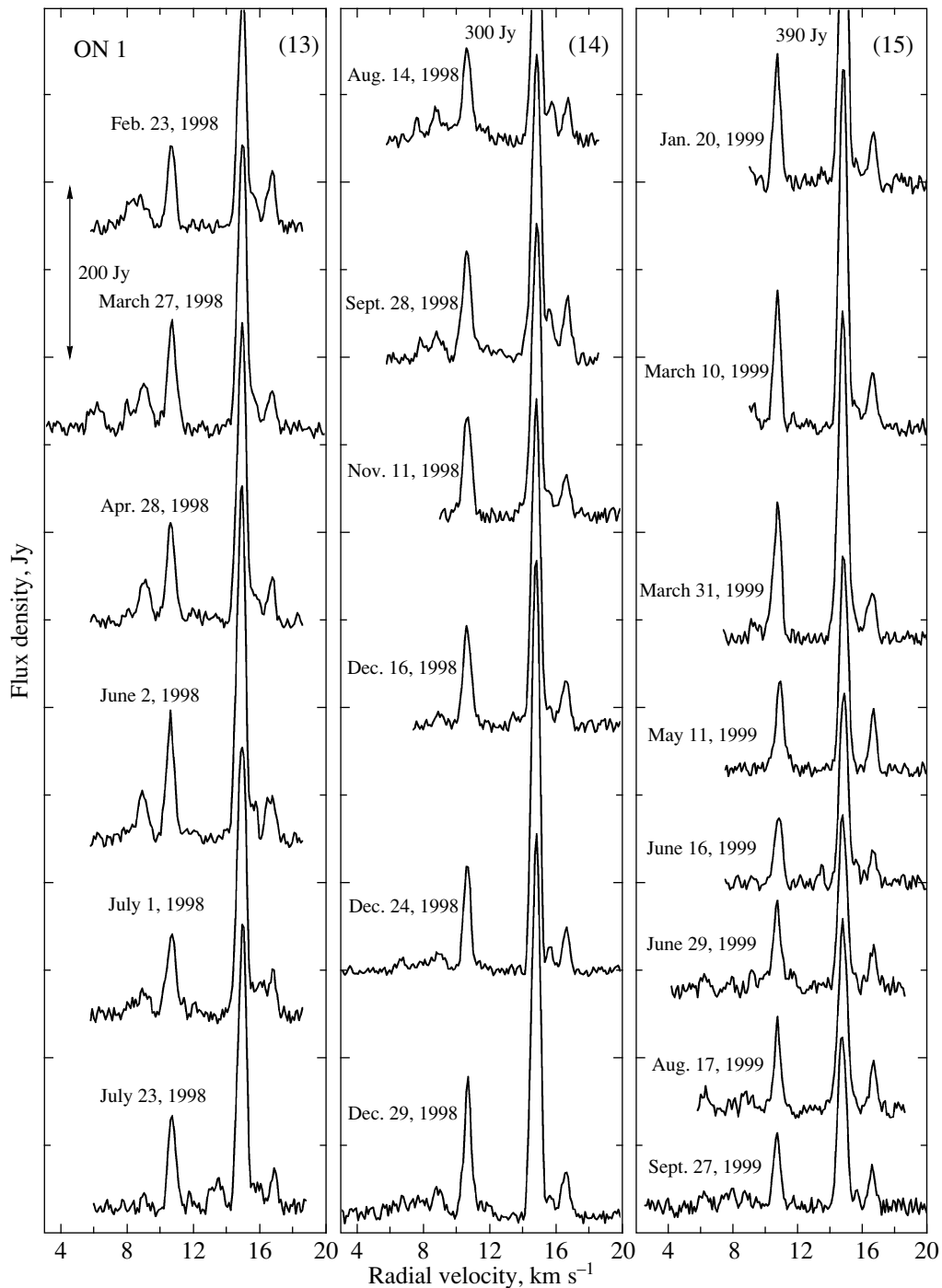


Fig. 1. (Contd.)

except the 1991 maximum, which was determined by the emission of only the component at 14.7 km s^{-1} and several weak features in the velocity range $4\text{--}14 \text{ km s}^{-1}$.

The emission of the emission features at 9.5 and 10.3 km s^{-1} was more or less periodic, with mean periods of 2.6 and 4.8 years, respectively. The former component most likely belongs to WMC 1 (Downes

et al. 1979) and the latter belongs to WMC 2 (Nagayama et al. 2008). No periodicity was found in the emission variability of the remaining components (see Fig. 6).

Thus, we can assert that no correlation is traced between the fluxes in individual spectral components. Consequently, the observed secondary maxima in Fig. 2 are most likely the effect of a superposition

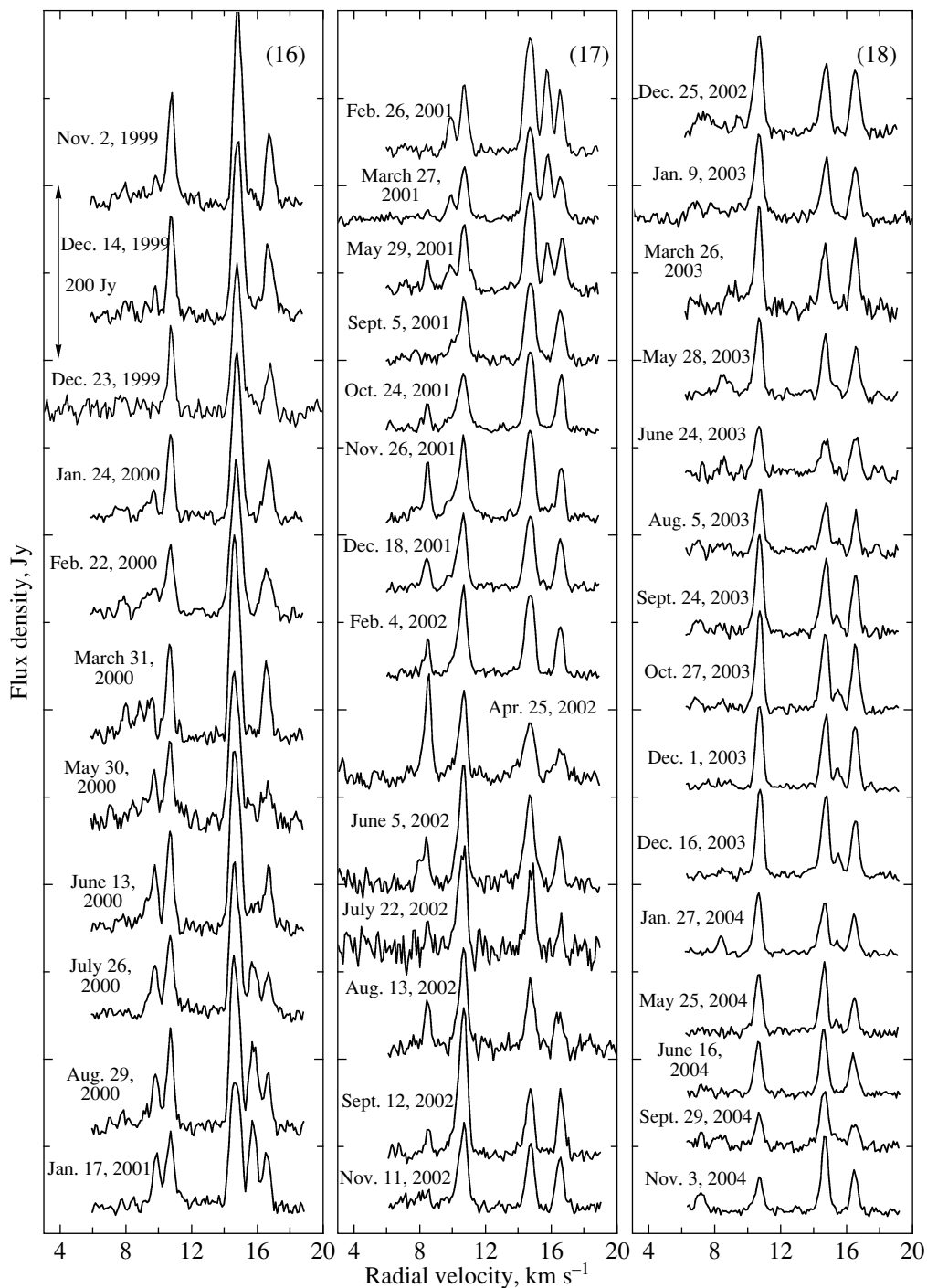


Fig. 1. (Contd.)

of the flux variability curves from several emission features at once on one another.

Let us return to Fig. 3. Three features with mean radial velocities of 10.5, 14.7, and 16.5 km s^{-1} stand out. Our analysis of the spectra showed that the pattern of the small drift in the radial velocities of these features is caused by the variability of the emission from several components with very close radial

velocities. For example, the feature in the spectrum at a mean velocity of 14.7 km s^{-1} actually consists of three components: 14.3, 14.7, and 15.4 km s^{-1} (see Fig. 3). In 1981–1982, a flare of the component at a velocity of 14.3 km s^{-1} occurred. Subsequently, only the component at 14.7 km s^{-1} was in an active stage for a long time, as is suggested by the very narrow

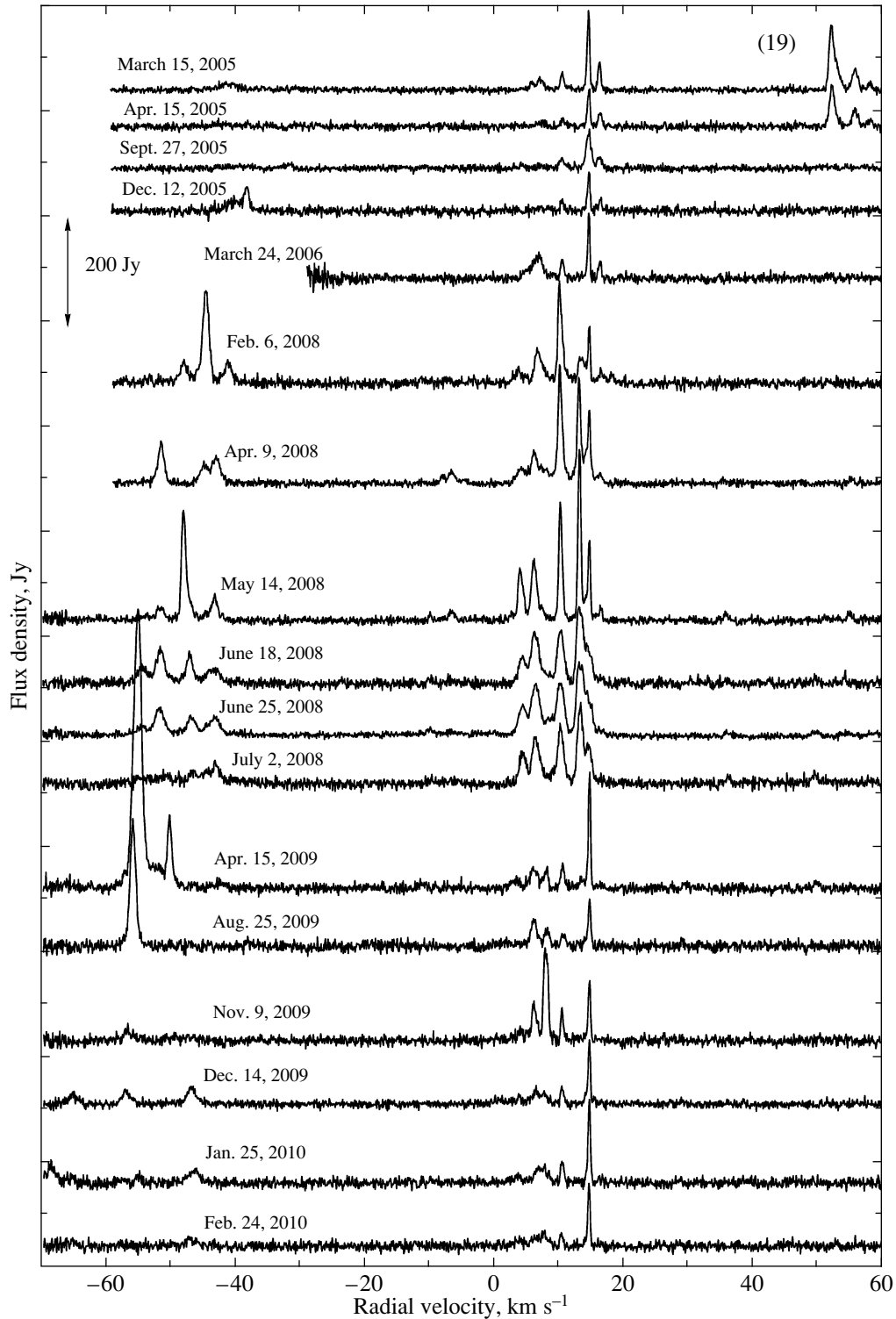


Fig. 1. (Contd.)

line width, only $0.6\text{--}0.7\text{ km s}^{-1}$. Weak emission from the other components was occasionally observed in the line wings or the line became asymmetric because of its blending with features close in velocity.

Similar pictures of evolution were also observed for the emission of the features at velocities of 14.3 and 16.5 km s^{-1} .

Thus, there is reason to believe that the emis-

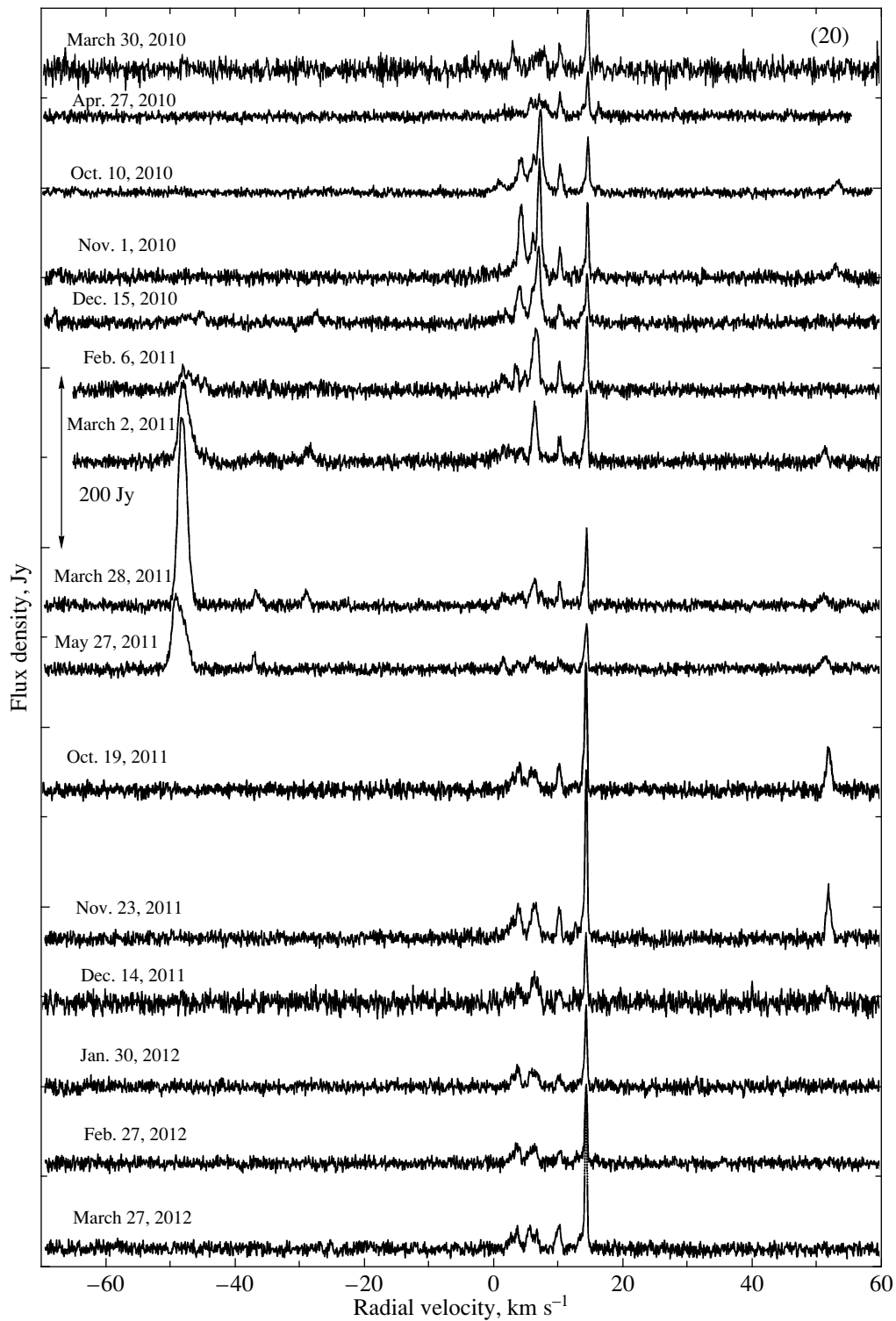


Fig. 1. (Contd.)

sion at these velocities belongs to compact structures formed by maser clumps belonging to WMC 1 and WMC 2 and having close radial velocities.

It should also be noted that the H₂O spectra ob-

served in 1976 (Forster et al. 1978) and 1977 (Genzel and Downes 1977) also exhibited emission features at 14.5 and 16.5 km s⁻¹. This shows that WMC 1 and WMC 2 are fairly stable structures over a long time.

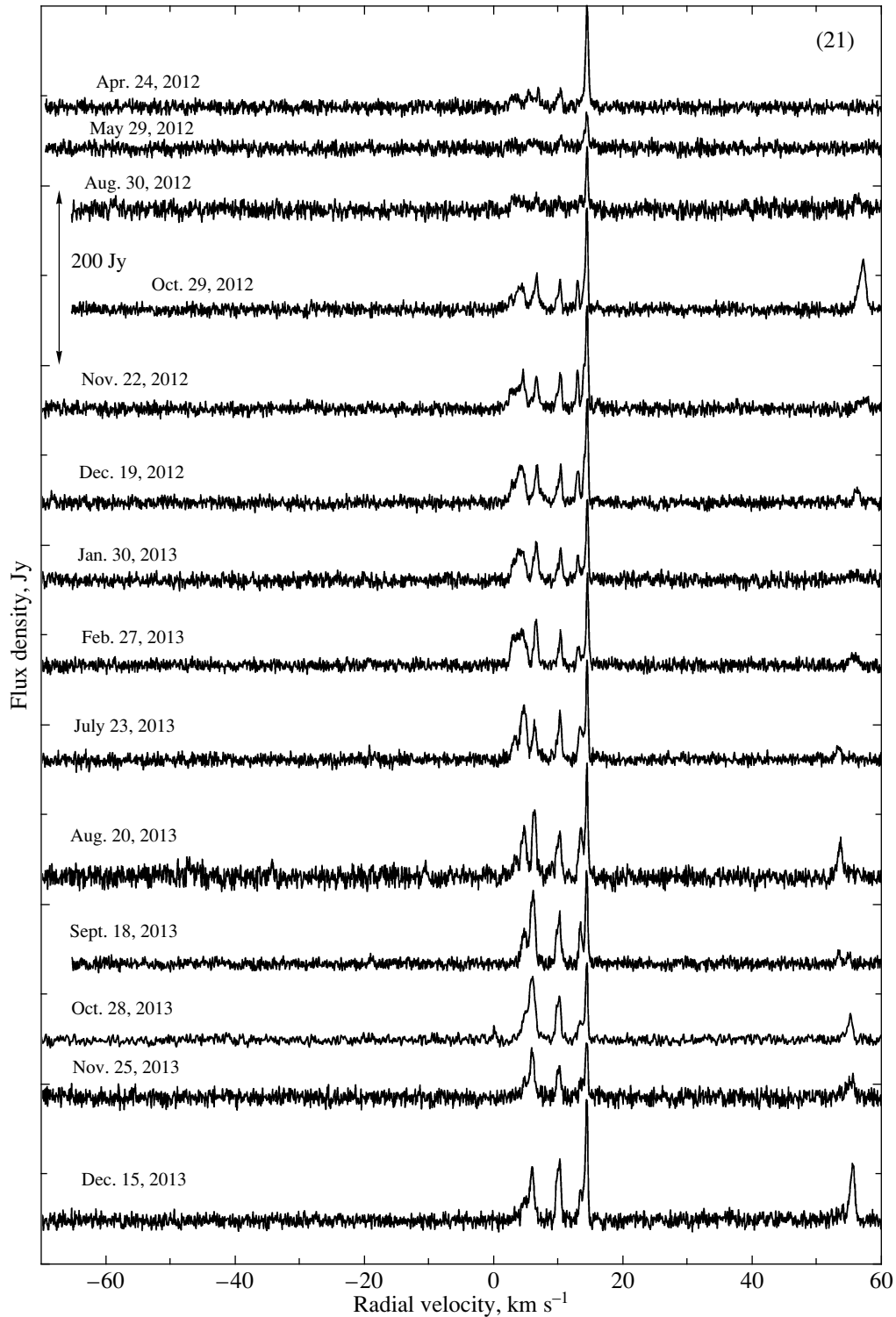


Fig. 1. (Contd.)

The High-Velocity Emission

We have traced the variability of the high-velocity emission since its detection. In 1977 and 1987, only the blue-shifted emission was observed. The results

of all the subsequent observations are presented in Fig. 4. We included the data from Felli et al. (2007) for the time interval 1987–2007 and the data of our monitoring from 2005 to 2013 (this work). The po-

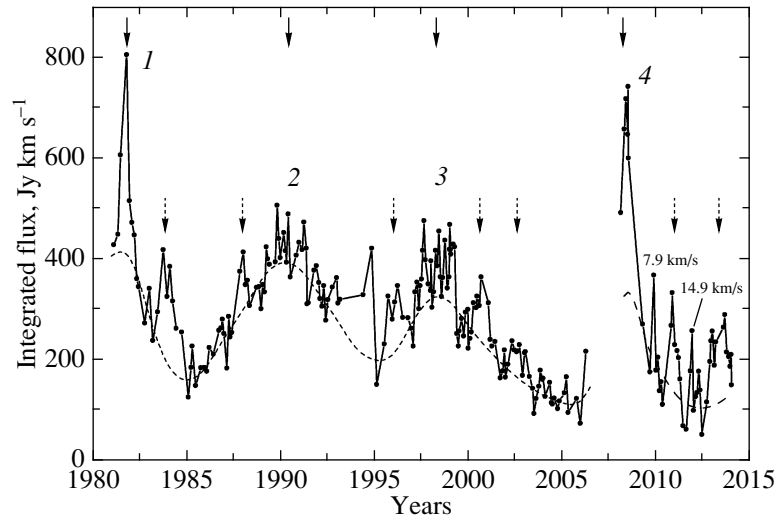


Fig. 2. Variability of the integrated flux of 1.35-cm H_2O maser emission in the range of radial velocities 4–18 km s^{-1} . The vertical solid arrows indicate the positions of the maxima. The dashed line indicate the slow variations. The dotted arrows mark the additional maxima.

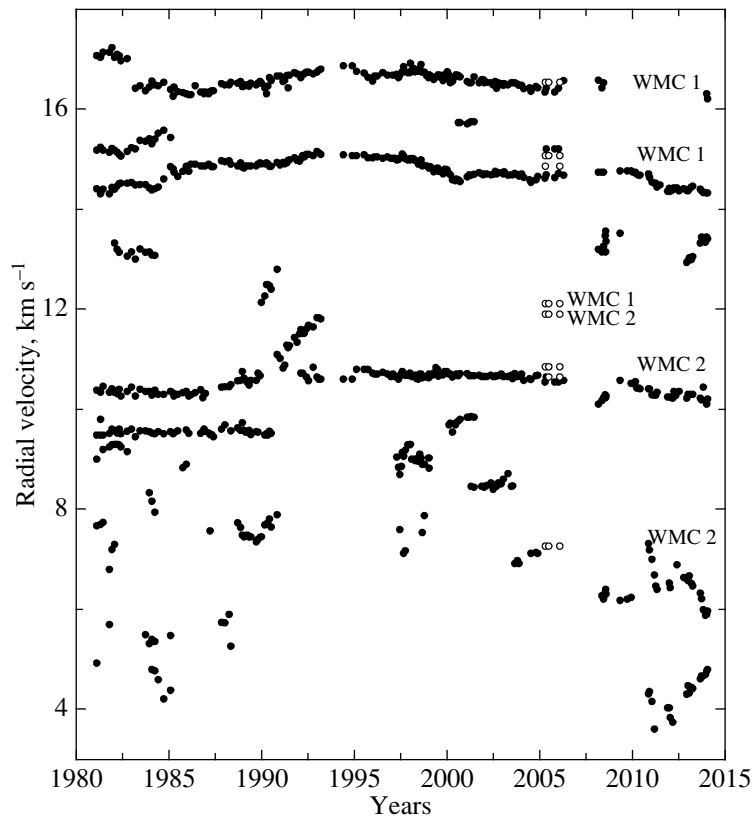


Fig. 3. Radial-velocity drifts of the main features. The open circles represent the data from Nagayama et al. (2008). The belonging of features to the clusters is marked on the right.

sitions of all the high-velocity emission features at all epochs of observations are indicated by the crosses. The features with flux densities exceeding 50 Jy are designated by different symbols (see Fig. 4). The

dashed lines indicate the drift of features with close radial velocities, and the dash-dotted line indicates the changes in the positions of the flare maxima with time.

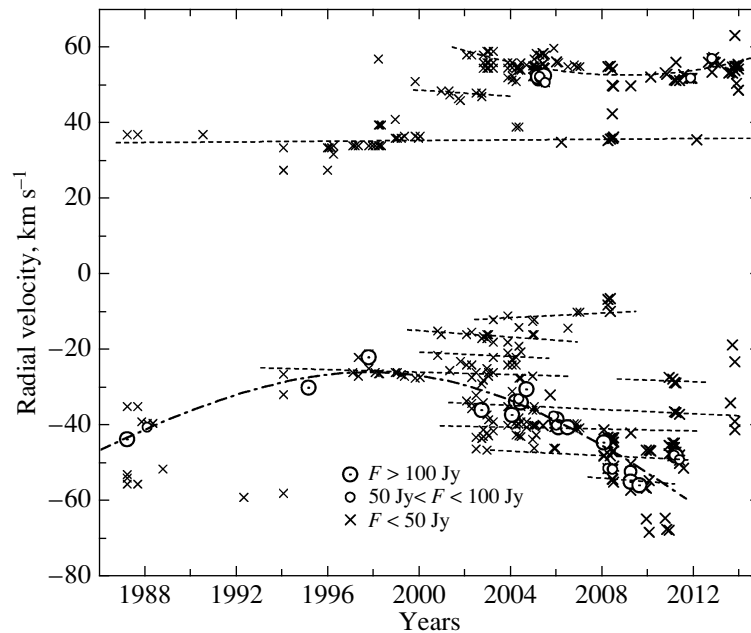


Fig. 4. High-velocity components of the H₂O maser emission. The flux densities of individual components are represented by the corresponding symbols shown in the lower part of the figure. The dashed lines indicate the drift of features with close radial velocities, and the dash-dotted line indicates the changes in the positions of the flare peaks with time.

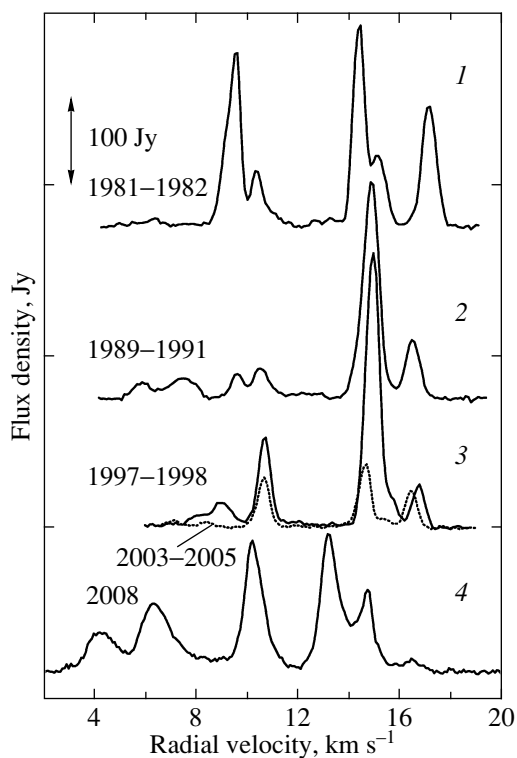


Fig. 5. Average H₂O spectra near the maxima. The averaging intervals and the maximum numbers are indicated. The dotted line indicates the average spectrum near the minimum in 2003–2005.

Our analysis of the spectra reveals rapid flux and radial-velocity variability for the high-velocity features. As a rule, the variability time scales were shorter than the intervals between successive observations. This does not allow us to estimate the parameters of the variability of individual emission features. In addition, weaker short-lived features appeared at radial velocities close to them.

The observed pattern of variability can be a consequence of strong fragmentation of the medium and the existence of small-scale turbulent motions of matter in the region where the high-velocity maser emission is localized.

The high-velocity features in ON 1 form two spatial groups that are located mainly in different parts of the outflow observed in the CO line. The features with negative velocities are located in the western part, while those with positive ones are located in the eastern part of the molecular outflow. According to Nagayama et al. (2008), the expansion velocity of this outflow is $\sim 69 \text{ km s}^{-1}$.

Our analysis of all data showed that the blue- and redshifted emission was observed from 1997 to November 2011. Subsequently, the emission was observed only at positive radial velocities (this work). No correlation is traced between the stages of maxima of the high-velocity and central ($2\text{--}20 \text{ km s}^{-1}$) emissions.

Thus, in contrast to the H₂O maser emission from WMC 1 and WMC 2, the maser emission from the

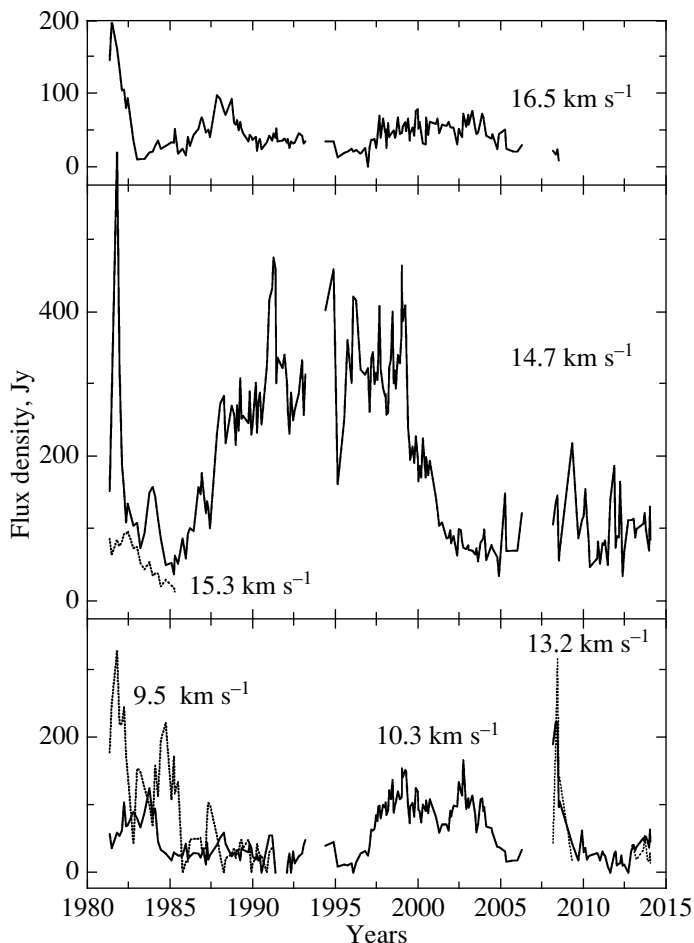


Fig. 6. H₂O emission variability of the main features. Their radial velocities are shown.

molecular outflow is characterized by rapid variability of individual features. The strong H₂O maser emission variability can be related to inhomogeneity of the material in the bipolar molecular outflow, to the presence of clusters of maser spots in it, and to small-scale turbulent motions.

Other Spectral Features

We also traced the evolution of the emission in the velocity range 20–25 km s⁻¹. This emission has been observed since the discovery of the maser in ON 1 (Turner et al. 1970; Sullivan 1973), i.e., in 1969–1970, and then in 1977 (Sullivan 1973; Genzel and Downes 1977). At the end of 1977, the emission features were observed in both clusters of maser spots. In 1987, the emission in the above velocity range was not recorded (Comoretto et al. 1990), nor was it recorded in succeeding years. In our monitoring, the observations in the range from 18 to 23 km s⁻¹ were conducted regularly from 1994 to 1996 and then, until 2005, only occasionally. We did not record any emission at these velocities either. On the other

hand, we have observed weak short-lived emission at various radial velocities, from –30 to 0 km s⁻¹ and from 35 to 40 km s⁻¹, since 2005.

Thus, H₂O maser emission from the source ON 1 was observed in a wide range of radial velocities, from –69 to +60 km s⁻¹. The fairly stable emission is associated with WMC 1 and WMC 2. It can be surmised that the short-lived emission we detected in the ranges from –30 to 0 and from 35 to 40 km s⁻¹, along with the high-velocity emission, is associated with the bipolar molecular outflow.

CONCLUSIONS

Let us summarize the main results of the 33-year-long monitoring of ON 1 in the 1.35-cm water-vapor line.

- (1) We constructed the H₂O maser emission spectra of ON 1 over the period 1981–2013.
- (2) Long-period variability of the integrated H₂O emission in the range of radial velocities 4–18 km s⁻¹ with a mean period of about 9 years was detected.

(3) The main emission features were identified with two clusters of maser spots, WMC 1 and WMC 2. According to Nagayama et al. (2008), the high-velocity emission (with both blue and red shifts) can be identified with a bipolar outflow observed in the CO line.

(4) The emission at velocities of 10.3, 14.7, and 16.5 km s⁻¹ is a superposition of individual emission features with close radial velocities, and these features apparently form compact structures in WMC 1 and WMC 2.

(5) Short-lived emission features were observed in the velocity ranges -30-0 and 35-40 km s⁻¹. We surmise that they are associated with the same bipolar outflow.

ACKNOWLEDGMENTS

This work was supported by the Ministry of Education and Science of the Russian Federation on the RT-22 radio telescope (registration number 01-10) as well as by the “Nonstationary Phenomena in Objects of the Universe” Program of the Presidium of the Russian Academy of Sciences and the “Active Processes in Galactic and Extragalactic Objects” Basic Research Program of the Division of Physical Sciences of the Russian Academy of Sciences. We wish to thank the staff of the Pushchino Radio Astronomy Observatory for their great help with the observations.

REFERENCES

1. A. L. Argon, M. J. Reid, and K. M. Menten, *Astrophys. J. Suppl. Ser.* **129**, 156 (2000).
2. G. Comoretto, F. Palagi, R. Cesaroni, M. Felli, A. Bettarini, M. Catarzi, G. P. Curioni, P. Curioni, et al., *Astron. Astrophys. Suppl. Ser.* **84**, 179 (1990).
3. D. Downes, R. Genzel, I. M. Moran, K. J. Johnston, L. I. Matveenko, L. R. Kogan, V. I. Kostenko, and B. Ronnang, *Astron. Astrophys.* **79**, 233 (1979).
4. M. Felli, J. Brand, R. Cesaroni, C. Codella, G. Comoretto, S. DiÈFranco, F. Massi, L. Moscadelli, et al., *Astron. Astrophys.* **476**, 373 (2007).
5. V. L. Fish, M. J. Reid, A. L. Argon, and X. W. Zheng, *Astrophys. J. Suppl. Ser.* **160**, 220 (2005).
6. J. R. Forster, W. J. Welch, C. H. Wright, and A. Baudry, *Astrophys. J.* **221**, 137 (1978).
7. R. Genzel and D. Downes, *Astron. Astrophys. Suppl. Ser.* **30**, 145 (1977).
8. M. S. N. Kumar, M. Tafalla, and R. Bachiller, *Astron. Astrophys.* **426**, 195 (2004).
9. S. Kurtz and P. Hofner, *Astron. J.* **130**, 711 (2005).
10. E. E. Lekht, E. Mendosa-Torres, R. L. Sorochenko, *Astron. Rep.* **39**, 34 (1995).
11. J. Lim, M. Choi, and P. T. Ho, *ASP Conf. Ser.* **267**, 385 (2002).
12. G. C. MacLeod, E. Scalise, Jr., S. Saedt, J. A. Galt, and M. J. Gaylard, *Astron. J.* **116**, 1897 (1998).
13. T. Nagayama, A. Nakagawa, H. Imai, T. Omodaka, and Y. Sofue, *Publ. Astron. Soc. Jpn.* **60**, 183 (2008).
14. Y. N. Su, S. Y. Liu, J. Lim, N. Ohashi, H. Beuther, Q. Zhang, P. Sollins, T. Hunter, T. K. Sridharan, J.-H. Zhao, and P. T. P. Ho, *Astrophys. J. Lett.* **616**, L39 (2004).
15. W. T. Sullivan III, *Astrophys. J. Suppl. Ser.* **25**, 393 (1973).
16. B. E. Turner, D. Buhl, E. B. Chrchwell, P. G. Mezger, and L. E. Snyder, *Astron. Astrophys.* **4**, 165 (1970).
17. X. W. Zheng, P. T. P. Ho, M. J. Reid, and M. H. Schneps, *Astrophys. J.* **293**, 522 (1985).

Translated by G. Rudnitskii